Novel PCM-based fin and tube heat exchanger system for building heating and cooling applications

Achutha Tamraparni, PhD
Member ASHRAE

Joe Rendall, PhD
Member ASHRAE

Zhenglai Shen, PhD
Member ASHRAE

Hevar Palani

Diana Hun, PhD
Member ASHRAE

Som Shrestha, PhD
Member ASHRAE

ABSTRACT

In the United States, the building sector accounts for 40% of all energy use, and buildings are responsible for more than two-thirds of electricity consumption. Buildings remain the major driver of energy-related carbon emissions, and such emissions are projected to increase in the years ahead because of urbanization and population growth. To accomplish the low carbon energy goal in the building sector, phase change material (PCM)–based thermal energy storage (TES) is increasingly being adopted because it offers several advantages, such as reducing building peak load and energy consumption, enabling large scale deployment of renewables, and improving grid stability.

The integration of TES with thermally anisotropic building envelopes (TABEs) is a promising solution because, TABE can redirect natural thermal energy from a building using hydronic loops to TES, and the stored energy can be used later for heating and cooling applications. In this study, we experimentally investigate the thermal performance of a novel fin-tube heat exchanger TES system designed for potential integration with a TABE. An experimental rig for a 5-gal PCM fin-tube heat exchanger system with water as the heat transfer medium is described which records temperatures at the heated and cooled boundaries of the system. Experimental observations provide insight into the role a TES system can play in offsetting a building's heating and cooling demand and also offer a means to characterize the performance of PCMs for building applications. The scale and study presented in this work will help in the design of future thermal storage systems optimized for storage capacity while also accounting for overall system costs for building applications.

INTRODUCTION

The building sector accounts for 75% of electricity and 40% of all energy use in the United States (Baldwin et al. 2015). The heating and cooling demands of buildings—such as heating, ventilation, and air-conditioning systems; water heating; and refrigeration—represent nearly 50% of total building energy consumption (Goetzler et al. 2017).

Achutha Tamraparni is a postdoctoral research associate, **Joseph Rendall** is a R&D associate staff member and **Zhenglai Shen** is a R&D associate staff member at the Oak Ridge National Laboratory, TN. **Hevar Palani** is a PhD student at University of Illinois, Chicago. **Diana Hun** is a Group Leader and **Som Shrestha** is a Senior R&D staff member at the Oak Ridge National Laboratory, TN.

Furthermore, heating and cooling of buildings account for more than 10% of global energy consumption and carbon dioxide emissions (Ürge-Vorsatz et al. 2015). Given the significance of thermal loads to building electricity consumption, thermally based storage technologies are vitally important in the pursuit of a clean energy economy and for managing energy for the built environment.

One critical factor that affects the space heating and cooling load is the building envelope, the structure that separates the indoor environment from the ambient conditions. To reduce building energy consumption, recent work developed a thermally anisotropic building envelope (TABE) system (Biswas et al. 2020). TABE consists of alternating layers of thermally conductive sheets of metal and insulation layers embedded in a building envelope to move heat or thermal energy in a preferred direction. The conductive metal layers are connected to hydronic loops, which collect natural thermal energy from diurnal weather conditions on the exterior side of the TABE roof (Shen et al. 2023). When TABE is coupled with a heat sink or source, recent findings for single-family residential buildings show annual savings of 19%–26% in cooling energy use and 13%–26% in heating energy use under weather conditions representative of Phoenix and Baltimore (Biswas et al. 2020).

While the application of TABE for building thermal management shows promise in reducing heating and cooling loads, one fundamental challenge to overcome is the mismatch of available natural thermal energy and building energy demand over a wide range of timescales. To help address this mismatch, thermal energy storage (TES) systems offer unique benefits by enabling time-shifted matching of building energy demand with the diurnal swings of the natural environment (Akeiber et al. 2016; Heier et al. 2015; Henry et al. 2020). The resulting flexibility from TES integration allows greater reliance on renewable sources, reduces costly grid reinforcement, and, more importantly, decarbonizes buildings by storing off-peak power (Al-Yasiri &Szabó 2021; Parameshwaran et al. 2012). Phase change materials (PCMs) having a large latent heat are promising for building thermal storage applications because they can absorb and release energy at a steady temperature (for pure single PCMs). Among the different classes of PCMs, solid-liquid PCMs are advantageous because of their large latent heat energy capacity, low volumetric changes between phases, and favorable transition temperatures. Although PCMs offer advantages of high energy density from their latent heat; the relatively low thermal conductivity of PCMs limits the system's power density and overall storage efficiency. One common method to increase the power density is to mix high-conductivity material with PCM, forming a composite structure in the form of particles, matrices, and fins (Agyenim et al. 2010; Fan &Khodadadi 2011; Shatikian et al. 2005). However, with the introduction of thermal conductivity materials, energy density of the PCM is reduced relative to pure PCM materials because metal conductors have low heat capacity, which creates a tradeoff between energy and power densities for thermal storage applications (Tamraparni et al. 2023; Woods et al. 2021).

As we consider thermal storage for building applications, it is important to evaluate the cooling power capacity or the heat transfer rates of PCM/metal thermal storage system. However, the nature of heat transfer in such systems is complex because the heat transfer in such systems is not an intrinsic material property but rather depends on the geometry, boundary condition, and magnitude and type of thermal load. In this work, we experimentally investigate the thermal performance of a 0.019 m^3 (5-gal) fin tube heat exchanger system designed for potential integration with TABE. For typical buildings, peak heating, and cooling loads last 3–4 hours. Here, we seek to design and optimize a thermal storage system that can utilize 90% PCM volume, with an objective to utilize 75% of the stored latent energy in 3 hours and 90% of the stored latent energy in 4 hours with a temperature difference of 5.55°C (10°F). Within the scope of this work, we first describe an experimental test apparatus, which allows for simultaneous heating and cooling of two 0.019 m^3 (5-gal) PCM heat exchangers. Second, we demonstrate a method to evaluate the energy storage capacity. Third, we report preliminary results from the test apparatus and provide a method to evaluate the thermal state of charge (SOC) of the PCM heat exchanger using the test apparatus. The demonstrated method can be used in the future to characterize the performance of PCM material and systems for building energy storage applications.

EXPERIMENTAL

Apparatus

The thermal energy storage capacity of a 5-gal PCM heat exchanger was evaluated using the experimental setup shown in Figure 1. Two 5-gal storage tank heat exchangers—shown as tank 1 and tank 2—were used to incorporate a fin and tube heat exchanger with PCM as the thermal storage medium.

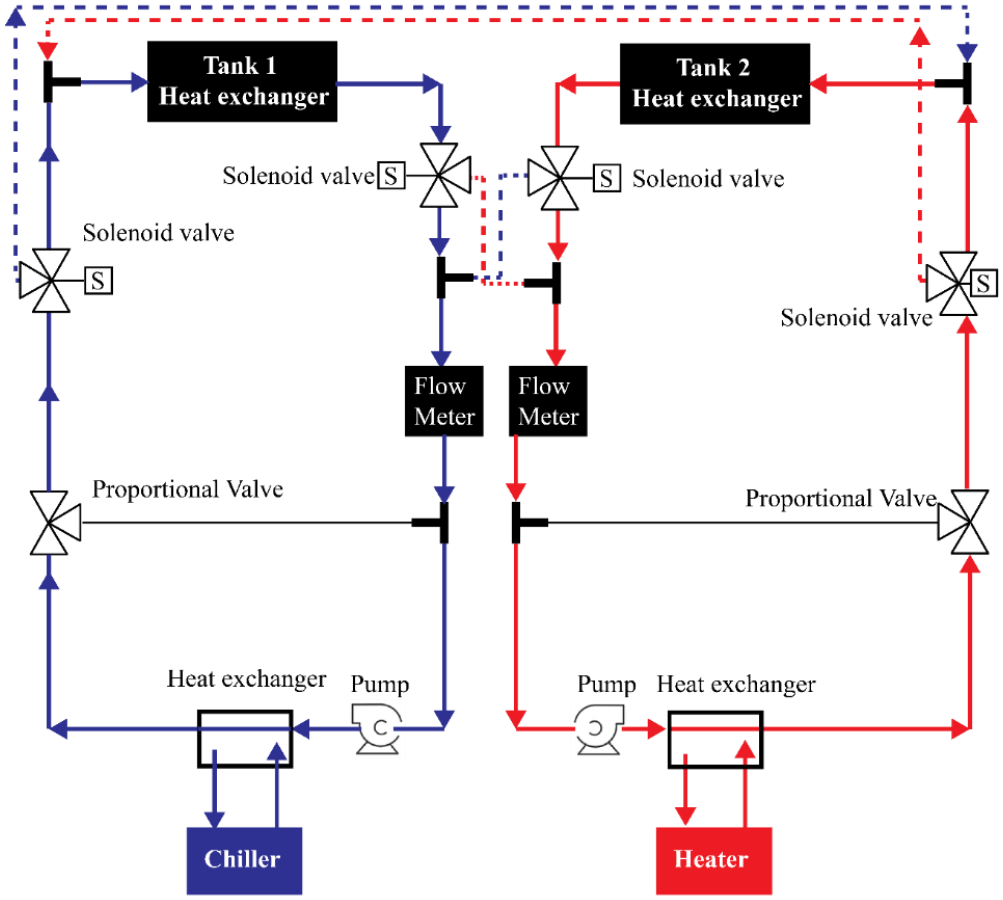

Figure 1 Schematic of the experimental setup for characterizing the performance of a 5-gal PCM heat exchanger system. Flow setup for the heat exchanger system shows a chiller and a heater supplying water for cooling and heating cycles, respectively, with solenoid valves to switch between the cycles. When solenoid valves are activated, flow from the chiller to the tank 1 heat exchanger is blocked and allowed to move to the tank 2 heat exchanger, as shown by the blue dotted line. Similarly, flow from the heater to the tank 2 heat exchanger is blocked and allowed to move to the tank 1 heat exchanger, as shown by the red dotted line. The return lines from the heat exchangers follow the dotted lines that pass through the flow meter and back to the heater or chiller for heating or cooling, respectively.

The storage medium in the heat exchanger has inlet/outlet manifold connections of copper tubing (0.635 cm [0.25 in.] tube size) that pass through the top plate of the tank. Water as the heat transfer medium was supplied to the inlet side of the tanks using centrifugal-type pumps, which were connected through a differential proportional valve and a three-way solenoid valve. Solenoid valves control heating and cooling cycles for the heat exchanger, whereas the proportional valve controls the flow rate of the water supplied to the thermal storage system. A paddlewheel-type water flow meter was used at the outlet of the heat exchanger to measure the flow rate of the water supplied to the system.

The flow meters were calibrated in situ using the gravimetric calibration method, where a known amount of water through the flow meter was captured for a given time. The measured volumetric flow rate was compared with flow meter readings, and the uncertainty in measurement for flow meters was ± 1% of the reading. Temperature sensors were used at the inlet/outlet connections of the tanks, and sensors with different probe lengths were also inserted into the tank through the top plate to measure the transient temperature response of the thermal storage medium. Uncertainty for the temperature sensors used in this study was ± 0.5°C, measured using a calibrated microbath. In this study, data were recorded using a data logger (CR3000, Campbell Scientific) for temperature and flow rate measurements. Additionally, solenoid valves were controlled through a relay to switch between heating and cooling for the thermal storage systems. A water chiller connected to a plate fin heat exchanger supplied cold water to the thermal storage system during the cooling cycle. For the heating cycle, a water bath circulator connected to the plate fin heat exchanger was used, as shown in Figure 1.

Method

For a cooling cycle in the tank 1 heat exchanger, the chiller was set at 17.4°C (63.32°F). It was used to allow cold water to flow to the heat exchanger inlet using the pump, flowing through the proportional and solenoid valve, exchanging heat with the storage medium, and then returning to the pump. Similarly, for a heating cycle in the tank 2 heat exchanger, the heater was set at 28.5°C (83.3°F) for hot water to flow to the inlet and then return to the pump, as shown in Figure 1. The switch between the cooling and heating cycles for tank 1 and tank 2, respectively, begins when the solenoid valve blocks flow from the chiller (for tank 1) and simultaneously allows water to flow from the heater to the inlet, as represented by the red dotted line in Figure 1. At the same time, the solenoid valve connected to tank 2 blocks the flow from the heater, allowing cold water from the chiller to enter, represented by the blue dotted line shown in Figure 1.

Figure 2 shows images of the fin and tube heat exchanger that was optimized for energy and power densities for building thermal storage. Within the scope of this paper, the design and optimization of the heat exchanger using PCM will not be described here but can be found in a recent study (Rendall et al. 2023). The heat exchangers were made with copper tubes (0.635 cm [0.25 inch] tube size, 7.8 cm [3.07 inch] tube spacing) and aluminum fins (1.5 cm [0.59 inch] fin spacing, 0.8 mm [0.031 inch] fin thickness). They have a total height of 30.48 cm (12 in.), length of 22.86 cm (9 in.), and breadth of 22.86 cm (9 in.). In this study we employed PCM with a phase change temperature of 23°C (73.4°F), which was filled into the tanks installed with the heat exchanger, as shown in Figure 2(C). The thermophysical properties of the PCM provided by the manufacturer are listed in Table 1.

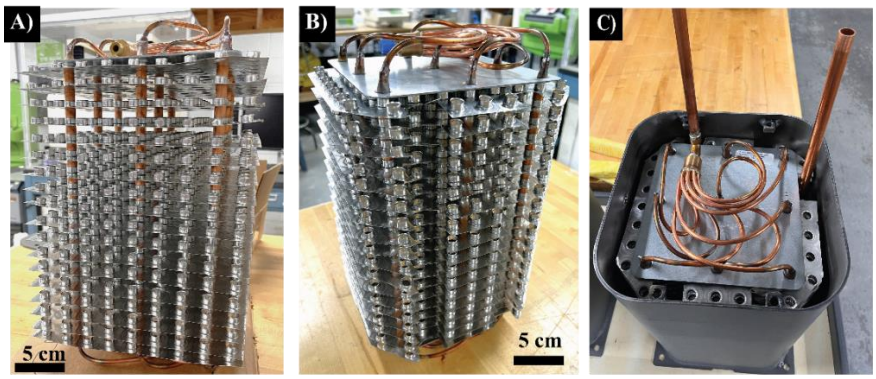

Figure 2 (A) Fin and tube heat exchanger used in this study. (B) Fins were altered at the sides to accommodate the heat exchanger inside the 5-gal tank. (C) Heat exchanger installed inside the tank with inlet and outlet connections.

Table 1. Thermophysical Properties of PCM

Material	Thermal Conductivity W/m-°C (Btu-in./h-ft²-°F)	Specific Heat J/g-°C (Btu/lb.-°F)	Latent Heat J/g (Btu/lb)	Melting Point °C (°F)	Density kg/m³ (lb/ft³)	Temperature Glide °C (°F)
PCM	0.15 (0.09) liquid, 0.25 (0.14) solid	1.99 (0.47) liquid, 1.84 (0.43) solid	201 (86.41)	23 (73.4)	830 (51.81) liquid, 910 (56.8) solid	2 (3.6)

RESULTS AND DISCUSSION

From the temperature recordings at the inlet and outlet of the heat exchanger, the rate of heat transfer (W) across the heat exchanger is calculated using

$$\dot{Q} = \dot{m} c_p (T_{in} - T_{out}) \tag{1}$$

where $\dot{m}$ is the mass flow rate measured from the mass flow meter (kg/s), c_p is the specific heat of water (J/kg °C), and T_{in} and T_{out} are the inlet and outlet temperatures (°C), respectively. Figure 3(a) shows the inlet and outlet temperatures recorded for the tank 2 heat exchanger with PCM during the heating cycle. When hot water enters the heat exchanger, it exchanges heat with PCM storage and returns through the outlet to the heater. As the heat front moves from the supplied hot water to the PCM storage, the outlet temperature shows a steady drop, as shown in Figure 3(a). Similarly, Figure 3(b) shows a gain in temperature for the tank 2 outlet during the cooling cycle. Using Equation (1), heat rates as a function of time for the heat exchanger were calculated as shown in Figure 3(c and d).

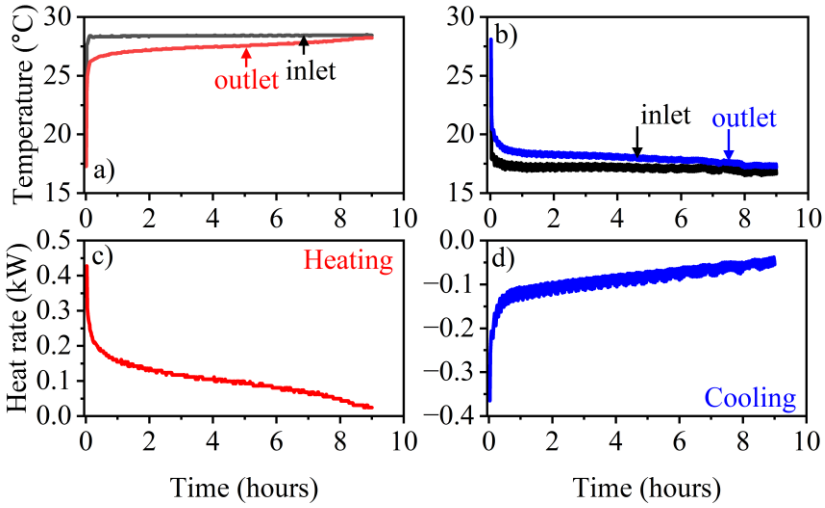

Figure 3 Plots of (a) inlet and outlet temperatures from the tank 2 heat exchanger with PCM when heating, (b) inlet and outlet temperatures when tank 2 is cooling, (c) heat rate as a function of time for tank 2 when heating, and (d) heat rate as a function of time for tank 2 when cooling.

The total thermal energy storage without considering the losses in the system can be calculated using

$$Q_{total} = \int_0^t \dot{Q} dt = \int_0^t \dot{m} c_p (\dot{T}_{in} - \dot{T}_{out}) dt \tag{2}$$

where Q_{total} is the total thermal energy stored without considering the losses in joules, and $\dot{Q}$ is the heating rate (W) calculated over total time t (in seconds) for the thermal storage media. To estimate heat losses in the system, we employed Newton's law of cooling, where the system at 40°C (104°F) was cooled to ambient temperature conditions. The temperature difference between the system tank and ambient as a function of time is shown in Figure 4.

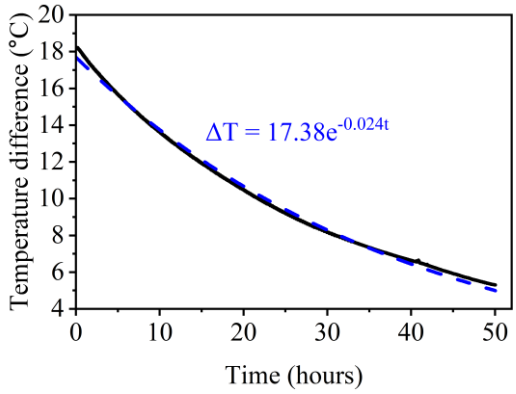

Figure 4 Temperature difference between the system tank and the ambient conditions as a function of time.

To estimate the heat loss from the TES tank, tank 1 was initially filled with water and connected to the water heater set at 40°C (104°F), followed by cooling of the system to ambient temperature conditions. We employed Newton's law of cooling, and the rate of heat loss from the tank to the environment was calculated by using Equations (3) and (4),

$$\Delta T = \Delta T_o e^{-\frac{t}{\tau}} \tag{3}$$

$$\tau = \frac{mc_p}{UA} \tag{4}$$

where ΔT is the temperature difference between the system and the environment measured in Celsius, ΔT_o is the temperature difference at time 0, t is the total time the system interacts with the environment in seconds, and τ is the time constant measured in seconds. The time constant can be further defined using Equation (4), where mc_p is the lumped total thermal capacitance (J/K) of the heat exchanger and water measured, U is the overall heat transfer coefficient(W/m²-K), and A is the total surface area of the TES system interacting with the environment measured in square meters. In this study, the heat loss rate of the system (UA) from Equation 4 is 0.5 W/K. Incorporating the heat loss into Equation (2), the total energy stored by the TES system can be calculated as

$$Q_{total,corrected} = \int_0^t \dot{Q}dt - UA(T(t) - T_{ambient}) \tag{5}$$

where $Q_{total,corrected}$ is the total energy stored for the TES system after correction in joules, $T_{ambient}$ is the indoor ambient temperature, and $T(t)$ is the tank temperature measured in Celsius.

In addition to inlet and outlet temperatures of the system, we also recorded temperature response from PCM thermal storage to estimate the overall energy storage capacity. Figure 5 shows the plot of temperature response from the PCM storage tank during heating and cooling. Temperature data in Figure 5 represent recordings from sensors at different spatial locations along the height of the tank, suspended in PCM storage. The results shown in Figure 5(a) indicate that variations in the onset of melting are primarily due to different heat rates experienced at different locations of the PCM. In general, temperature sensors close to the heat exchanger undergo melting, whereas melting times are longer for regions away from the fins, as shown in Figure 5(a). Figure 5(b) shows a similar behavior in temperatures,

where variations in the PCM storage are due to the slower heat transfer rates farther from the fins. Additionally, we observe subcooling behavior in the temperature response, followed by an increase in temperature; this could possibly be attributed to the freeze front from the PCM pushing the probes toward the fins and/or warmer regions of the PCM, thereby resulting in a slight increase in temperatures.

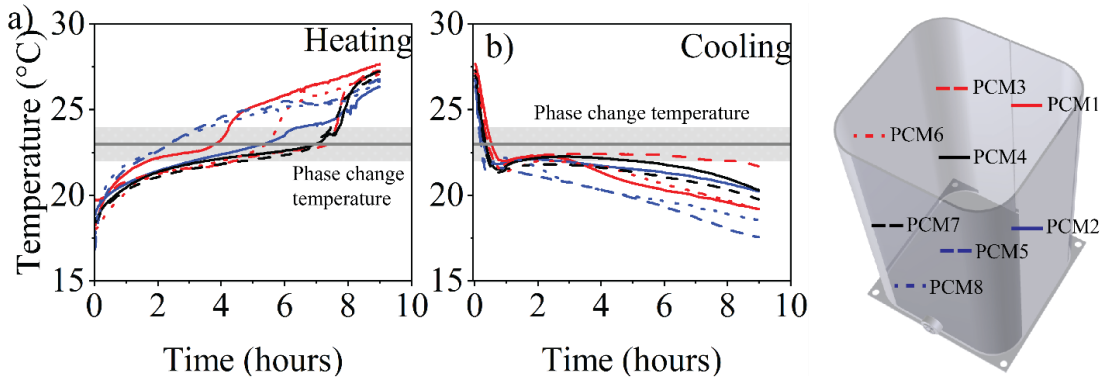

Figure 5 Plots of (a) temperature vs. time for PCM storage media during the heating cycle and (b) PCM temperatures from the PCM tank the during cooling cycle. Temperature data were recorded from locations at the top, middle, and bottom, along the height of the PCM tank – measured from the bottom surface to the top of the PCM tank.

Furthermore, using Equation (5) of total energy stored and the heat loss from the system, the thermal state of charge (SOC) for the system can be estimated as

$$SOC = \frac{Q_{total,corrected} - Q_{HX} - Q_{pcm,specific}}{C_{max}} \quad (6)$$

$$Q_{HX} = \int_0^t m_{hx} c_{p,HX} dT dt \quad (7)$$

$$Q_{pcm,specific} = \int_0^t m_{pcm} c_{p,HX} dT_{pcm} dt \quad (8)$$

where Q_{HX} is the total energy stored by the heat exchanger thermal mass in joules, $Q_{pcm,specific}$ is the specific heat energy stored up to the PCM transition temperature (in joules), and C_{max} is the maximum thermal energy storage capacity (joules) defined by the total mass of PCM multiplied by the PCM latent heat capacity. In addition, m_{hx} represents the measured mass of the heat exchanger (2.45 kg [5.4 lb.]), $c_{p,HX}$ is the specific heat of the heat exchanger (0.8 kJ/kg-K [0.191 Btu/lb.-°F]), m_{pcm} is the mass of PCM in the tank (kg), and dT_{pcm} is defined as the temperature difference measured from the transition temperature (Celsius) of the PCM.

Using Equations (6)–(8), we evaluate the SOC for the system at 0.0000252 m³/s (0.4 GPM) flow rate and a temperature difference of 5.55°C (10°F) as shown in Figure 6. The SOC is of interest because it provides critical information on charging and discharging rates that is highly useful when designing for building thermal storage applications. Here we observe that the system used around 5 and 6.5 hours to discharge 75% and 90% of the stored latent energy, respectively. To further improve the discharge or charge performance, the heat transfer rate between the PCM and heat exchanger can be improved by increasing the thermal conductivity of PCMs and/or increasing the fin spacing. Furthermore, selecting PCMs with large latent heat storage, compatibility of the PCM with the heat exchanger, and cyclic stability of the PCM have to be considered, when adopting new PCM materials. As a result, this approach creates a tradeoff between TES system thermal performance and cost per energy stored ($/kWH), because the cost of additional fins relative to high conductivity PCMs must be considered. In future work, we will seek to increase the flow rate of the system to increase the rate of charge or discharge in an effort to meet the desired goals of 75% discharge of

stored latent energy in 3 hours and 90% discharge of stored latent energy in 4 hours.

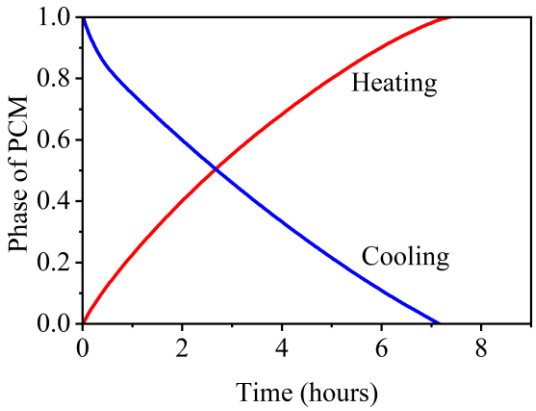

Figure 6 Phase of PCM evaluated as a function of time for heating and cooling at 0.0000252 m^3/s (0.4 GPM) and temperature difference of 5.55°C (10°F) with respect to the PCM transition temperature. (Note: This evaluation was with an insulation level that resulted in 0.5 W/K heat exchange with ambient conditions.)

CONCLUSION

This paper developed and demonstrated a medium-scale 5-gal thermal storage system, which integrates a novel fin and tube heat exchanger with a solid/liquid phase change material, for potential integration with a thermally anisotropic building envelope system. Preliminary results for the thermal storage system showed that the state of charge of the system using a phase change material with a phase change temperature of 23°C (73.4°F) was 75% in 5 hours; furthermore, 90% of the stored energy was discharged in 5 hours when evaluated at a temperature difference of 5.55°C (10°F) with respect to the PCM transition temperature. To further improve the discharge or charge performance, the heat transfer rate between the PCM and heat exchanger can be improved by increasing the thermal conductivity of PCMs and/or increasing the fin spacing. The experimental apparatus and methodology described in this study can be used for future systems to determine the PCM/heat exchanger performance, ultimately maximizing economic and environmental benefits through thermal storage in buildings.

ACKNOWLEDGMENTS

The authors would like to acknowledge Sven Mumme, Technology Manager, DOE Building Technologies Office, for his support and guidance.

NOMENCLATURE

A = area, m^2 (ft^2)
c_p = specific heat capacity, J/g-°C (Btu/lb-°F)
m = mass, kg (lb)
$\dot{m}$ = mass flow rate, kg/s (lb/h)
Q = total energy stored, J (Btu)
T = temperature, °C (°F)
t = time, s (h)
U = overall heat transfer coefficient, W/m^2-K (Btu/h-ft^2-°F)
τ = time constant, s (h)

Subscripts

HX = heat exchanger
pcm = phase change material
max = maximum
in = inlet
out = outlet
total = total energy stored

REFERENCES

Agyenim, F., Hewitt, N., Eames, P., and Smyth, M. 2010. A review of materials, heat transfer and phase change problem formulation for latent heat thermal energy storage systems (LHTESS). *Renewable and Sustainable Energy Reviews 14*(2): 615-628.

Akeiber, H., Nejat, P., Majid, M. Z. A., Wahid, M. A., Jomehzadeh, F., Famileh, I. Z., Calautit, J. K., Hughes, B. R., and Zaki, S. A. 2016. A review on phase change material (PCM) for sustainable passive cooling in building envelopes. *Renewable and Sustainable Energy Reviews 60*: 1470-1497.

Al-Yasiri, Q., and Szabó, M. 2021. Incorporation of phase change materials into building envelope for thermal comfort and energy saving: A comprehensive analysis. *Journal of Building engineering 36*: 102122.

Baldwin, S., Bindewald, G., Brown, A., Chen, C., Cheung, K., Clark, C., Cresko, J., Crozat, M., Daniels, J., and Edmonds, J. 2015. Quadrennial technology review: an assessment of energy technologies and research opportunities. *US Department of Energy: Washington, DC, USA*.

Biswas, K., Shrestha, S., Hun, D. E., and Atchley, J. 2020. Thermally Anisotropic Composites for Heat Redirection and Thermal Management in Building Envelopes. *Oak Ridge National Lab.(ORNL), Oak Ridge, TN (United States)*.

Fan, L., and Khodadadi, J. M. 2011. Thermal conductivity enhancement of phase change materials for thermal energy storage: a review. *Renewable and Sustainable Energy Reviews 15*(1): 24-46.

Goetzler, W., Shandross, R., Young, J., Petritchenko, O., Ringo, D., and McClive, S. 2017. Energy savings potential and RD&D opportunities for commercial building HVAC systems. *Navigant Consulting, Burlington, MA (United States)*.

Heier, J., Bales, C., and Martin, V. 2015. Combining thermal energy storage with buildings–a review. *Renewable and Sustainable Energy Reviews 42*: 1305-1325.

Henry, A., Prasher, R., and Majumdar, A. 2020. Five thermal energy grand challenges for decarbonization. *Nature Energy 5*(9): 635-637.

Parameshwaran, R., Kalaiselvam, S., Harikrishnan, S., and Elayaperumal, A. 2012. Sustainable thermal energy storage technologies for buildings: A review. *Renewable and Sustainable Energy Reviews 16*(5): 2394-2433.

Rendall, J., Shen, Z., Tamraparni, A., Hun, D., and Shrestha, S. 2023. Low-cost fin-tube heat exchanger design for building thermal energy storage using phase change material *Journal of energy storage Under Review*.

Shatikian, V., Ziskind, G., and Letan, R. 2005. Numerical investigation of a PCM-based heat sink with internal fins. *International Journal of Heat and Mass Transfer 48*(17): 3689-3706.

Shen, Z., Shrestha, S., Howard, D., Feng, T., Hun, D., and She, B. 2023. Machine learning–assisted prediction of heat fluxes through thermally anisotropic building envelopes. *Building and Environment 234*: 110157.

Tamraparni, A., Hoe, A., Deckard, M., Zhang, C., Malone, N., Elwany, A., Shamberger, P. J., and Felts, J. R. 2023. Design and optimization of composite phase change material for cylindrical thermal energy storage. *International Journal of Heat and Mass Transfer 208*: 123995.

Ürge-Vorsatz, D., Cabeza, L. F., Serrano, S., Barreneche, C., and Petrichenko, K. 2015. Heating and cooling energy trends and drivers in buildings. *Renewable and Sustainable Energy Reviews 41*: 85-98.

Woods, J., Mahvi, A., Goyal, A., Kozubal, E., Odukomaiya, A., and Jackson, R. 2021. Rate capability and Ragone plots for phase change thermal energy storage. *Nature Energy 6*(3): 295-302.